Clays and Clay Minerals, Vol. 48, No. 1, 120–131, 2000.

INFRARED STUDY OF WATER SORPTION ON Na-, Li-, Ca-, AND Mg-EXCHANGED (SWy-1 AND SAz-1) MONTMORILLONITE

WEIZONG XU,[1] CLIFF T. JOHNSTON,[1] PAUL PARKER,[1] AND STEPHEN F. AGNEW[2]

[1]Crop, Soil and Environmental Sciences, Agronomy Department, Purdue University, West Lafayette, Indiana 47907-1150, USA

[2]CST4, MS J586, Los Alamos National Laboratory, Los Alamos, New Mexico 87545, USA

Abstract—An environmental infrared microbalance (EIRM) cell was used to study H_2O sorption on two montmorillonite samples as a function of water content and type of exchangeable cation. The vibrational spectra showed that H_2O sorbed to the clay at low-water content was strongly influenced by the exchangeable cation and by the close proximity to the clay surface. At water contents <6 H_2O molecules per exchangeable cation, the H-O-H bending mode of H_2O (ν_2 mode) shifts to a lower frequency and is characterized by an increase in molar absorptivity. In contrast, the positions of the asymmetric and symmetric OH-stretching modes of sorbed water (ν_1 and ν_3 modes) shift to higher energies. These observations indicate that H_2O molecules sorbed to the clay surface at low-water content are less hydrogen bonded than in bulk H_2O. In addition, the vibrational-stretching and bending bands of the structural OH groups of the 2:1 layer are also strongly influenced by H_2O content and type of exchangeable cation. By using the EIRM cell, the molar absorptivities of the structural OH-bending vibrations were measured as a function of H_2O content. The position and molar absorptivity of the structural OH-bending bands at 920, 883, and 840 cm^{-1} are strongly influenced by H_2O content and type of exchangeable cation. The molar absorptivity of the 920-cm^{-1} band, which is assigned to the AlAlOH group, decreased strongly at low-H_2O content. This reduction in intensity is assigned to a dehydration-induced change in orientation of the structural OH groups resulting from the penetration of H_2O molecules into siloxane ditrigonal cavities that are not associated with a net negative charge from isomorphous substitutions.

Key Words—Exchangeable Cation, FTIR, Hydration, Hysteresis, Smectite, Sorption, Water.

INTRODUCTION

The influence of smectite surfaces on the chemical and physical properties of adsorbed H_2O molecules has been the subject of recent studies using structural, thermodynamic, spectroscopic, and computational methods. In recent structural studies of H_2O sorption on montmorillonite, for example, Cases and co-workers (Cases *et al.,* 1992, 1997; Berend *et al.,* 1996) provided conclusive evidence that the structure of the clay mineral quasi-crystals depends strongly on the exchangeable cation and H_2O content. This work showed that water adsorption proceeds by initial solvation of the exchangeable cations followed by the occupancy of remaining interlayer space. Thus, the hydration characteristics of the clay mineral depend strongly on the exchangeable cation. This conclusion is also supported by recent computational studies of smectite-H_2O complexes (Skipper *et al.,* 1991, 1995a, 1995b; Karaborni *et al.,* 1996; Chang *et al.,* 1997), and microcalorimeter data (Cancela *et al.,* 1997), which are strongly dependent on the type of interlayer cation.

Infrared spectroscopy (IR) provides a useful method to explore H_2O-cation-smectite interactions (Poinsignon *et al.,* 1978; Sposito and Prost, 1982; Johnston *et al.,* 1992), as H_2O can be used as a molecular probe of the smectite-water interface. The stretching and bending vibrations of H_2O are ideally suited to probe the short-range interactions of hydrated cations with the clay surface. In an IR study of smectite-H_2O interactions, Johnston *et al.* (1992) examined the effect of exchangeable cations on the position and molar absorptivity of the ν_2 mode of H_2O sorbed on smectite surfaces as a function of H_2O content. At low-H_2O content (<6 H_2O molecules per exchangeable cation), the H-O-H bending band shifted to lower energy and the molar absorptivity of this band was sharply increased compared to those of bulk water. The shift in frequency and change in molar absorptivity were strongly dependent on H_2O content, and on the type of the exchangeable cation. Cu^{2+}-exchanged SAz-1 showed the largest influence compared to Na^+, K^+, or Co^{2+}. These results indicated that the properties of H_2O molecules surrounding exchangeable cations near the surface at the interlayer were distinct from those of bulk water and were strongly influenced by the exchangeable cation.

The main objective of this paper is to examine a broader range of the IR-spectral region to include the OH-stretching and bending bands of H_2O and the IR bands of the smectite. Russell and Farmer (1964) showed that the intensity of the structural OH-bending bands increased for the fully hydrated Na- and Li-exchanged smectites compared to the same clays under dry conditions. Similar results were reported by Calvet and Prost (1971) for Li, Mg, Ca, and K-exchanged montmorillonite at different H_2O contents. They attributed the change in intensity to movement of the exchangeable cations into the ditrigonal cavities on the

siloxane surface of the smectite followed by reorientation of the structural OH groups within the 2:1 layer by the influence of the exchangeable cation. A similar argument was invoked by Sposito *et al.* (1983) to explain changes in IR intensities of structural OH-bending bands of reduced-charge Na-rich montmorillonites heated in the presence of Li. Under dry conditions, the intensities of the structural OH-bending vibrations at 920, 840, and 800 cm^{-1} were strongly reduced relative to the intensities at 50% relative humidity. The spectra provided clear evidence that the structural OH-bending vibrations of smectite were strongly influenced by H_2O content, although the amount of H_2O sorbed on the clay was not determined. The change in IR intensity of the structural OH-bending bands was attributed to the repulsive interaction between the exchangeable cation and OH groups. Recently, Alba *et al.* (1998) used the change in the intensity of the structural OH-bending bands, in conjunction with ^{29}Si, ^{27}Al, and ^{7}Li magic angle spinning nuclear magnetic resonance (MAS-NMR), X-ray diffraction (XRD), and thermal analysis, to study the behavior of Li^+ ions in the interlayer of montmorillonite. These studies provide direct evidence that exchangeable cations and the accompanying H_2O molecules influence the vibrational modes of the structural OH groups.

Although changes in the IR spectra of smectite-water complexes have been reported, few studies have quantitatively determined the amount of H_2O present. Most often, H_2O contents have been described qualitatively, for example, as a smectite sample equilibrated at a particular relative humidity, in a vacuum, or at elevated temperature (Calvet and Prost, 1971; Sposito *et al.,* 1983). In several IR studies of smectite-H_2O interactions, H_2O contents were determined *ex situ* (Mortland and Raman, 1968; Poinsignon *et al.,* 1978; Yan *et al.,* 1996a), where H_2O contents and spectroscopic properties were measured either separately or indirectly.

In this study, an environmental infrared microbalance (EIRM) cell was designed to allow IR spectra and water-vapor sorption isotherms to be obtained simultaneously. The combination of IR spectroscopy and gravimetric analysis provides three unique benefits. First, the EIRM cell provides a direct method to correlate changes in the molecular properties of H_2O sorbed on the clay with the macroscopic sorption behavior. Second, because the amount of smectite and sorbed water are known precisely, the molar absorptivities of both smectite and H_2O IR bands can be determined. Finally, the dry mass of the smectite sample can be determined accurately without drying to completeness which is required for conventional sorption isotherms.

MATERIALS AND METHODS

Preparation of self-supporting clay films

The samples studied were SAz-1 (Cheto montmorillonite, Apache County, Arizona), and SWy-1 (montmorillonite, Crook County, Wyoming) obtained from the Source Clays Repository of The Clay Minerals Society (van Olphen and Fripiat, 1979). SAz-1 is a high-charge montmorillonite [cation-exchange capacity (CEC) = 120 $cmol_c\ kg^{-1}$] with isomorphic substitution in the octahedral sheet only. The structural formula for SAz-1 is $M^{+}_{1.2}[Si_8][Al_{2.67}F\ e_{0.15}Mg_{1.20}]O_{20}(OH)_4$ (Breen *et al.,* 1995). SWy-1 is a low-charge montmorillonite (CEC = 80 $cmol_c\ kg^{-1}$) with substitution in both the octahedral and tetrahedral sheets. The structural formula (Weaver and Pollard, 1973) is $M^{+}_{0.62}[Si_{7.80}Al_{0.20}][Al_{3.28}Fe(III)_{0.3}Fe(II)_{0.04}Mg_{.38}]O_{20}(OH)_4$. Prior to size fractionation, a homoionic montmorillonite suspension was prepared by placing 10 g of the clay in 1.0 L of 0.5 M NaCl. The resulting suspension was washed free of excess salts by repeated centrifugation with distilled-deionized water. The <0.5-μm size fraction was collected by centrifugation. Near-homoionic clay suspensions of Na-, Li-, Ca-, or Mg-exchanged smectite were prepared by adding, respectively, ~0.7 L of 0.05 M solution of the metal chloride to the salt-free clay suspension (volume ~0.3 L), such that the total volume was 1.0 L. The washing and size-fractionation steps were completed within a 24-h period to minimize degradation of the clay.

Self-supporting clay films were prepared by washing 20 mL of the stock montmorillonite suspensions free of excess salts. The solids concentration of the suspension was diluted to 2.5 mg clay/g of suspension. Aliquots of this suspension were deposited on a polyethylene sheet and allowed to dry. The dry clay films were peeled off the polyethylene sheet as self-supporting clay films. The resulting self-supporting clay films had a cross-sectional density of 2–3 mg per cm^2 of film surface. For details, see Johnston *et al.* (1992) and Johnston and Aochi (1996).

EIRM cell

Fourier transform infrared (FTIR) spectra were obtained using a Perkin-Elmer model 1600 spectrometer equipped with a DTGS detector and a KBr beamsplitter. The spectrometer was controlled by using the Grams Analyst software. The unapodized resolution for the FTIR spectra was 2.0 cm^{-1}, and 64 scans were signal averaged for each spectrum. Spectra were collected using an EIRM cell (Figure 1). The cell consists of a 15-cm pathlength gas cell fitted with two ZnSe windows and sealed by Viton O-rings. The cell is connected to a Cahn Model RG electrobalance. The EIRM cell allowed FTIR spectra and gravimetric data to be collected simultaneously. Unlike previous FTIR/gravimetric studies, the relative pressure of water-vapor in the EIRM cell was controlled using a flowing-gas manifold instead of vacuum methods (Johnston *et al.,* 1992; Tipton *et al.,* 1993). The cell was connected to a flowing-gas manifold using two MKS mass-flow controllers to regulate the flow of wet (100% relative

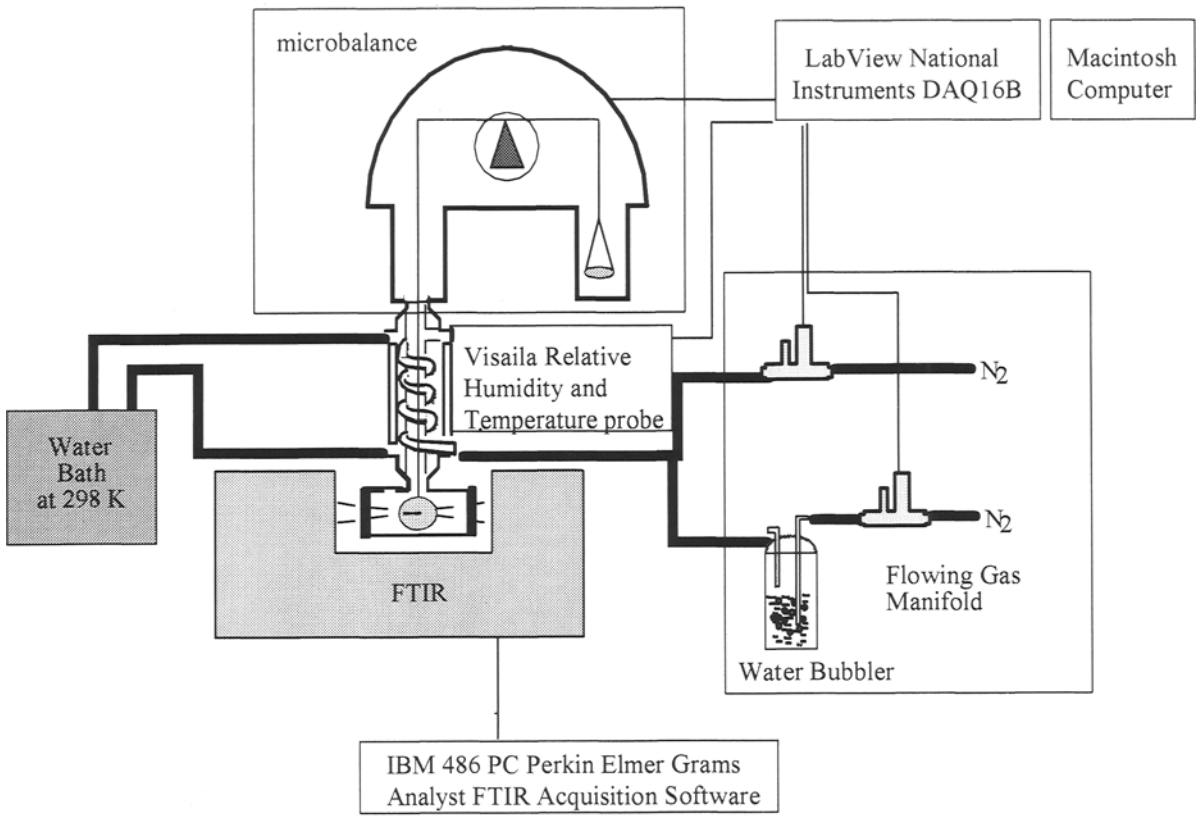

Figure 1. Schematic diagram of the EIRM. The apparatus consists of a Cahn microbalance designed to hold self-supporting films of smectite in a 15-cm pathlength gas cell. The cell is fitted with two 50 × 3-mm ZnSe windows. The gas cell is mounted in the sample compartment of a Perkin Elmer Model 1600 FTIR Spectrometer.

humidity of N_2) and dry N_2. The flow rate was constant at 100 sccm (std cm^3 min^{-1}) and the relative proportions of the wet and dry N_2 were adjusted to maintain a specified relative humidity. Relative humidity was monitored on-line using a Vaisala model HMP35A humidity probe.

Self-supporting homoionic montmorillonite films were placed on a 0.2-mm Pt hangdown wire suspended from the weighing arm (Figure 1) of the Cahn electrobalance. Four cm^2 square self-supporting films (~10 mg) were cut from larger clay films to minimize edge effects. The clay films were suspended from the weighing arm of the electrobalance while ~150 mg of standard weight were placed on the tare arm of the electrobalance to compensate for the mass of the film, holder, and hangdown wire. A wire-frame holder constructed from 0.2-mm Pt wire allowed the clay film to lie flat and perpendicular to the incident IR beam. Self-supporting clay films of montmorillonite tend to curl during dehydration and this holder kept the clay films flat. The EIRM cell and FTIR spectrometer were mounted on a NRC optic table to mechanically isolate the electrobalance assembly.

Spectra were analyzed with the Grams spectral analysis software (version 4.1, Galactic software) using a nonlinear *least-squares* routine. For the H-O-H bending region of H_2O, a single band of mixed Gaussian and Lorentzian lineshape was used to fit the 1630-cm^{-1} band. Based on Johnston *et al.* (1992), fitting the H-O-H bending band to more than one band was not justified. In the OH-stretching region from 3100 to 3700 cm^{-1}, four bands at 3630, 3580, 3420, and 3250 cm^{-1} were used to fit the experimental data. A similar set of bands was used by Madejova *et al.* (1996). For the 3580-cm^{-1} band, the intensity was varied but not the position and linewidth. In the structural OH-bending region of 1000–800 cm^{-1}, spectra were fit using three bands at 920, 880, and 840 cm^{-1}. For each spectral region, a linear baseline correction was used and the spectra were fit using a lineshape of variable Gaussian-Lorentzian character.

To examine hysteresis, water-vapor adsorption-desorption isotherms were obtained for Ca, Mg, or Na-exchanged SAz-1 and for Na-exchanged SWy-1. For all other samples, only the desorption portion of the isotherm was obtained. These experiments were based on the observation by Mooney *et al.* (1952a, 1952b) that whereas desorption isotherms are reproducible, adsorption isotherms are not. Kijne (1969) reported similar results and attributed the availability of starting

https://doi.org/10.1346/CCMN.2000.0480115 Published online by Cambridge University Press

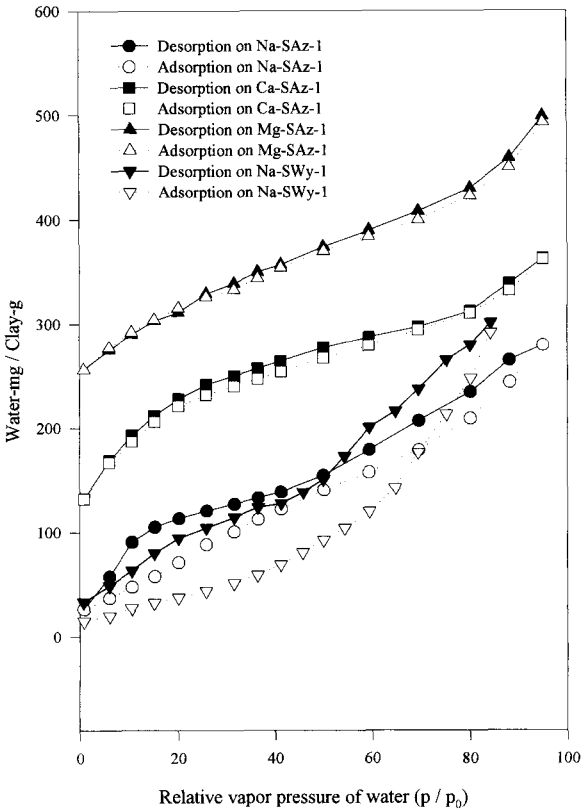

Figure 2. Water-vapor desorption-adsorption isotherms from self-supporting films of Na-, Ca-, and Mg-exchanged SAz-1 montmorillonite, and a Na-exchanged SWy-1 montmorillonite.

water content to this water-adsorption behavior. For both adsorption-desorption experiments, the samples were equilibrated with a high relative pressure of H_2O (~0.95) for 4 h, the mass of the sample was recorded from the microbalance, and the FTIR spectrum of the clay film was collected. The relative pressure of H_2O of the flowing gas was reduced by increments of 0.1 or 0.05 units by controlling the relative proportions of the dry N_2 and H_2O-saturated N_2 gas. At a given relative pressure of H_2O, the sample was allowed to equilibrate for 2 h, the vapor pressure was recorded, and the FTIR spectrum of the sample was collected. This procedure was repeated until dry N_2 gas was flowing over the sample, which corresponded to a measured relative vapor pressure of ~0.02. For adsorption isotherms, the partial pressure of H_2O was increased following the same data collection methods.

RESULTS

Water-vapor sorption isotherms

Water-vapor adsorption-desorption isotherms for Ca-, Mg-, and Na-exchanged SAz-1 and Na-exchanged SWy-1 are presented in Figure 2. In addition, water-vapor desorption isotherms were obtained for Li-, Ca-, and Mg-exchanged SWy-1 and Li-exchanged SAz-1. As noted by Mooney *et al.* (1952a, 1952b), adsorption isotherms are critically dependent on the starting H_2O content of the sample and, in general, are not reproducible. In contrast, desorption isotherms were found to be reproducible. Unless otherwise noted, the data presented here correspond to desorption isotherms. Little hysteresis is observed for the more strongly hydrated cations (Mg^{2+} and Ca^{2+}). However, significantly greater hysteresis was observed for the Na-exchanged sample. The degree of hysteresis is in agreement with previous water-vapor sorption studies (Mooney *et al.*, 1952a, 1952b; Berend *et al.*, 1996) with significantly more hysteresis for Na^+-exchanged than for Ca^{2+} or Mg^{2+}-exchanged smectites. The desorption branches of these isotherms are in reasonable agreement with published water-vapor desorption isotherms (*e.g.*, Cases *et al.*, 1997).

IR spectra of smectite-H_2O complexes

FTIR spectra were obtained along the water-vapor desorption-adsorption isotherms as illustrated for the water-vapor desorption isotherm for Ca-exchanged SAz-1 (hereafter Ca-SAz-1, and similarly, Ca-exchanged SWy-1 is hereafter Ca-SWy-1, *etc.*) shown in Figure 3. The spectral regions of interest are the OH-stretching region (Figure 3b), H-O-H bending region of H_2O (Figure 3c), and the structural OH-bending region of the structural OH groups (Figure 3d). Sorbed water contributes to the H-O-H bending region (1600–1650 cm^{-1}) and to the O-H stretching region (3000–3700 cm^{-1}). In comparison, the structural OH groups contribute to the FTIR spectra in the OH-deformation region (800–1000 cm^{-1}) and to the O-H stretching region.

ν_2 band of sorbed water (H-O-H bending). The position (Figure 3c) of the H-O-H bending band of water (ν_2 mode) is plotted as a function of H_2O content for self-supporting films of SAz-1 and SWy-1 exchanged with Li, Na, Ca, or Mg in Figure 4. The spectral data and water-content values reported in Figures 4 correspond to data collected from the desorption branch of the sorption isotherms. The position of the ν_2 mode of H_2O sorbed on smectite at concentrations of >30 H_2O molecules per cation is ~1635 cm^{-1}, which compares to a value of 1643.5 cm^{-1} for bulk water (Venyaminov *et al.*, 1997). The ν_2-band position remains constant at concentrations of 30–45 H_2O molecules per cation. For Na or Li-exchanged smectites, lowering the concentrations to ~6 H_2O molecules per exchangeable cation results in band shifts to a slightly higher value by 1–2 cm^{-1}. This is followed by a decrease in frequency to values of 1625 cm^{-1} (Na-SWy-1) and 1629 cm^{-1} (Na-SAz-1) upon further reduction of H_2O content. For Ca- or Mg-exchanged SWy-1, the position of the ν_2 band showed little change in frequency as a

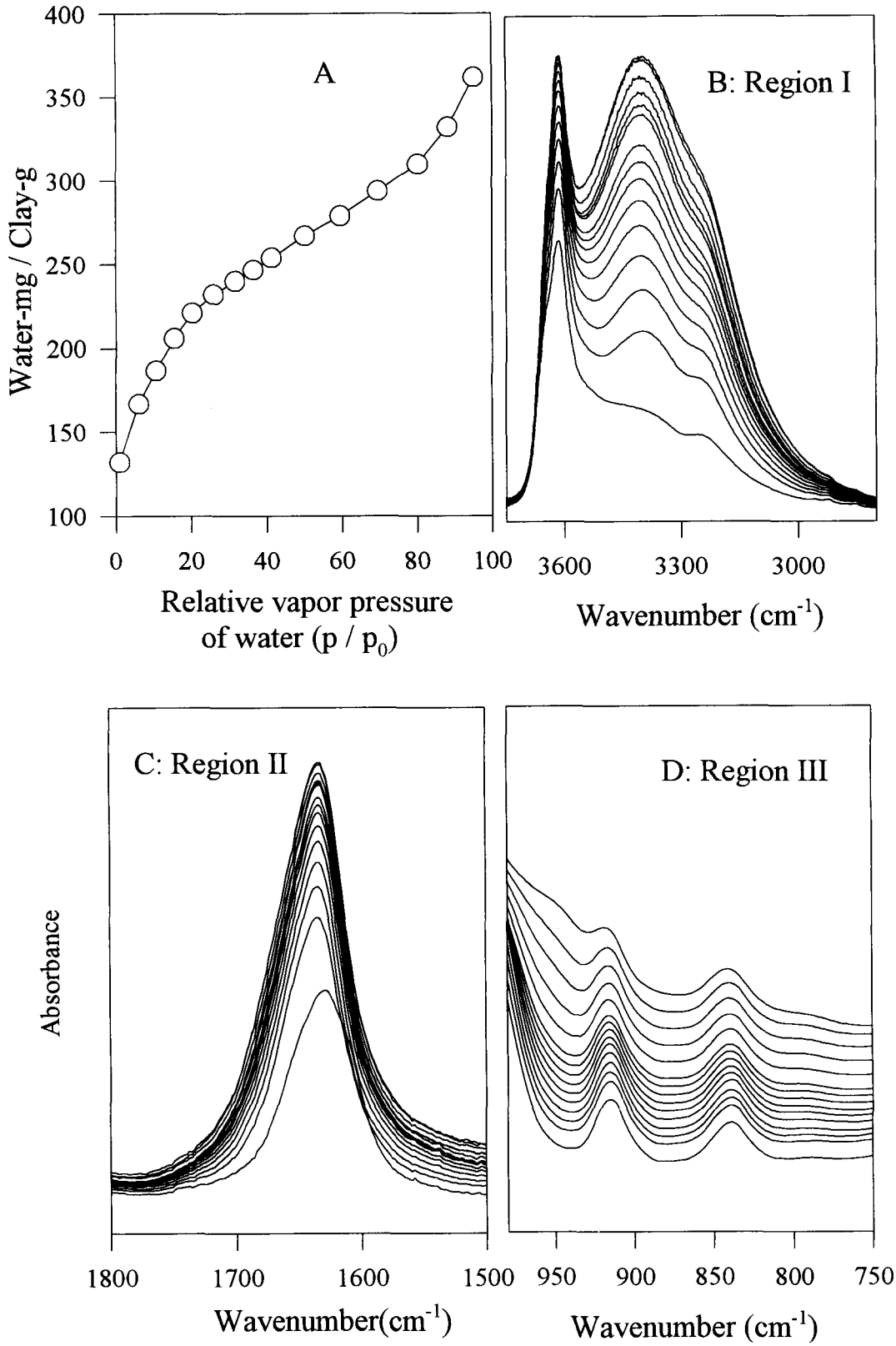

https://doi.org/10.1346/CCMN.2000.0480115 Published online by Cambridge University Press

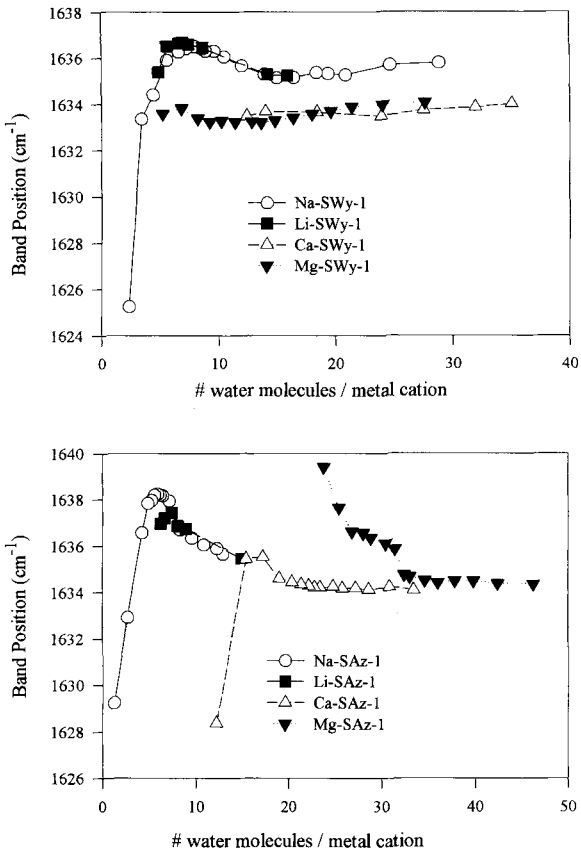

Figure 4. Position of the H-O-H bending vibration of H_2O (ν_2) as a function of H_2O content for Na-, Li-, Ca-, and Mg-exchanged SWy-1 (top) and SAz-1 (bottom) montmorillonite.

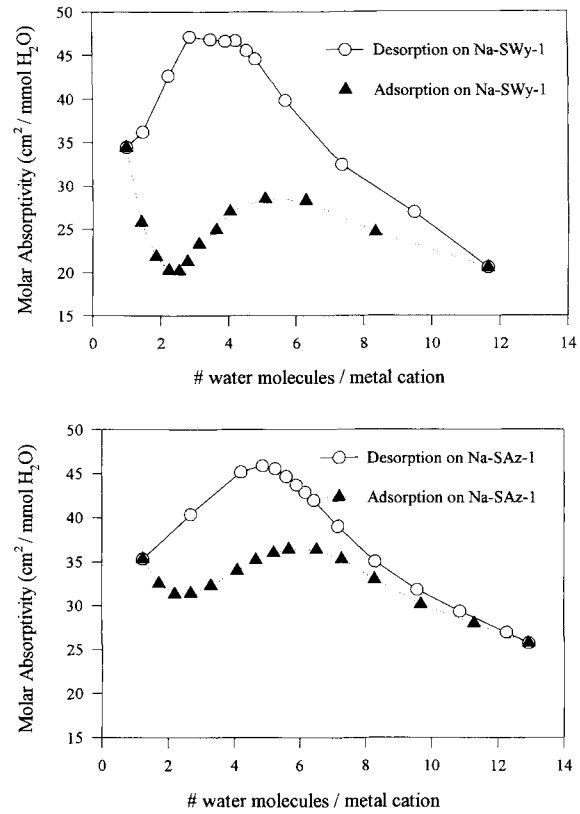

Figure 5. Hysteresis of molar absorptivity (cm^2/mmol H_2O) of the H-O-H bending vibration of H_2O (ν_2) observed during the desorption and adsorption portions of the H_2O-sorption isotherms for Na-exchanged SWy-1 (top) and SAz-1 montmorillonite (bottom).

function of H_2O content. In contrast, large shifts in the position of the ν_2 band of H_2O were observed for Ca or Mg-SAz-1. Upon lowering the H_2O content of Mg-SAz-1, the position of the ν_2 band increased by ~5 cm^{-1}. For Ca-SAz-1, the position of the ν_2 band increased slightly, followed by a decrease to 1628 cm^{-1}.

Hysteresis of the ν_2 mode upon wetting and drying. The molar absorptivity of the ν_2 band of H_2O was determined based upon the amount of H_2O sorbed and the measured absorbance value using

$$A(\nu) = \epsilon(\nu)cd \quad (1)$$

$$A(\nu) = \epsilon(\nu)\hat{c} \quad (2)$$

the Bouguer-Beer-Lambert law ("Beer's law"). As described in Johnston *et al.* (1992), $A(\nu)$ is the absorbance of the band of interest, $\epsilon(\nu)$ is the molar absorptivity at wavenumber ν and has units of M^{-1} cm^{-1}, c is the molar concentration of water (M), d is the thickness of the clay film in cm, and $\hat{c}$ is the amount of H_2O sorbed per unit area of clay film (moles cm^{-2}). Using the EIRM cell, $A(\nu)$ and $\hat{c}$ can be measured directly, allowing the value of $\epsilon(\nu)$ to be determined according to Equation (2).

Similar to the hysteresis shown in the water-vapor sorption isotherms (Figure 3), a hysteresis effect is also shown clearly by the change in molar absorptivity of the ν_2 band of H_2O upon dehydration and rehydration of Na-SAz-1 and Na-SWy-1 (Figure 5). Upon lowering the H_2O content, the molar absorptivity of the ν_2 band of H_2O increases until a critical value of ~4–6 H_2O molecules per exchangeable cation is

←

Figure 3. Water-vapor desorption isotherm from a Ca-exchanged self-supporting film of SAz-1 at 298 K obtained using the EIRM cell (A). For each point along the water-vapor desorption isotherm a corresponding FTIR spectrum was obtained using the EIRM cell. In the top right portion (B), the FTIR spectra of the OH-stretching region in the 3800–2800-cm^{-1} region are shown as a function of H_2O content. FTIR spectra in the OH-bending region of H_2O (C; 1800–1500 cm^{-1}) and the structural OH-bending region (D; 1000–750 cm^{-1}) are shown in the lower portion.

https://doi.org/10.1346/CCMN.2000.0480115 Published online by Cambridge University Press

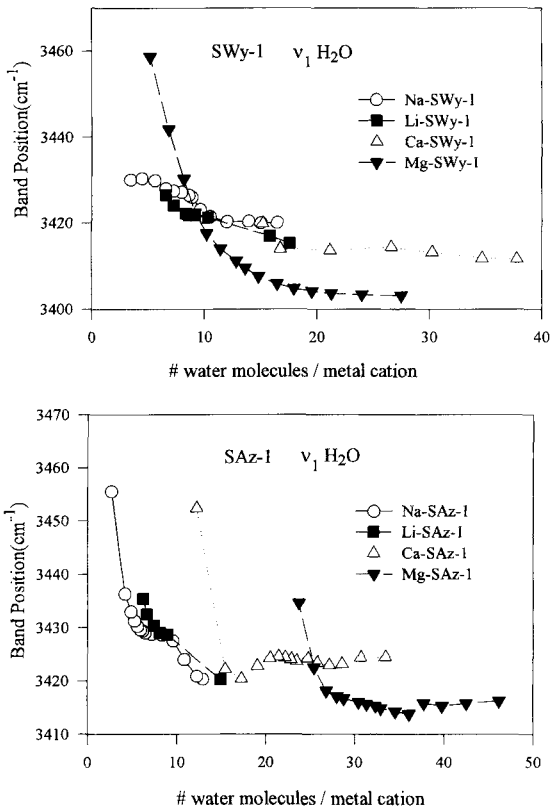

Figure 6. Position of the ν_1 ν(O-H) stretching vibration of H_2O as a function of H_2O content for Na-, Li-, Ca-, and Mg-exchanged SWy-1 (top) and SAz-1 (bottom) montmorillonite.

reached. Upon further dehydration, the molar-absorptivity values decrease. These results are in good agreement with previously reported molar absorptivities of the ν_2 band obtained from water *desorption* isotherms of Na-SAz-1 (Johnston *et al.*, 1992). A strongly contrasting trend, however, is shown in the molar-absorptivity values of the ν_2 band of H_2O obtained from the *adsorption* leg. In this case, the addition of H_2O to the dry clay results in an initial decrease in the molar absorptivity, followed by an increase. Strong hysteresis occurred for both Na-SWy-1 and Na-SAz-1, although somewhat greater hysteresis was observed for Na-SWy-1 (Figure 5).

ν(O-H) region. IR spectra in the region of 3800–2700 cm^{-1} for smectite-H_2O complexes are characterized by a relatively sharp band at 3630 cm^{-1} corresponding to the ν(O-H) band of structural OH groups and three broad bands at 3580, 3420, and 3250 cm^{-1} corresponding to the OH-stretching bands of sorbed water. The positions of the 3420-cm^{-1} band of water sorbed on Na-, Li-, Ca-, and Mg-SAz-1 and SWy-1 samples are plotted as a function of H_2O content in Figure 6. The dehydration-induced shifts in frequencies of these bands are opposite to that of the ν_2 (H-O-H bend). The highest frequency component at the 3580 and 3420-cm^{-1} bands are assigned to the ν_3 and ν_1 ν(OH) bands of water, respectively. The band at 3250 cm^{-1} is an overtone of the ν_2 band. Upon lowering the H_2O content, the peak position of the ν_1 band increases in frequency by values to $\leq$60 cm^{-1}. The position of the ν_1 ν(OH) band for Mg-exchanged SWy-1 is ~3403 cm^{-1} at high-H_2O content. This compares to a position of 3413 cm^{-1} for Mg-exchanged SAz-1.

Structural OH modes. SAz-1 is characterized by two dominant structural OH-bending vibrations at 915 and 840 cm^{-1} corresponding to the AlAlOH and AlMgOH groups, respectively. In contrast, SWy-1 has three bands at 920, 885, and 845 cm^{-1} which are assigned to the structural OH-bending vibrations of AlAlOH, $AlFe^{3+}OH$ and AlMgOH groups, respectively (Farmer, 1974). The band positions of the structural OH-bending bands of SAz-1 and SWy-1 are plotted as a function of H_2O content in Figure 7. In all cases, the structural OH-bending bands exhibited small frequency shifts of $\leq$5 cm^{-1}. For SWy-1, the position of the 920-cm^{-1} band remained nearly constant. The 885 and 845-cm^{-1} bands, however, upon dehydration shift in opposite directions by 3–4 cm^{-1}. The 885-cm^{-1} band decreased as a function of decreasing H_2O content from a value of ~885 to 883 cm^{-1} (Figure 7). In contrast, the 845-cm^{-1} band increased in frequency to 849 cm^{-1}. A similar increase in frequency was observed for the 840-cm^{-1} band of SAz-1, which increased in frequency by two wavenumbers upon dehydration.

More apparent than the change in frequency, however, was the dehydration-induced reduction in IR intensity of the structural OH-deformation bands. The EIRM cell was used to measure the molar absorptivities of the *smectite* bands themselves. The molar absorptivities of the structural OH-bending vibrations of self-supporting films of SAz-1 and SWy-1 are shown in Figure 8. We believe that these data represent the first direct determination of the molar absorptivities of the structural OH-deformation bands of a clay mineral. In agreement with previously reported qualitative observations (Calvet and Prost, 1971; Sposito *et al.*, 1983), large variations of molar absorptivity were observed for the structural OH-bending bands. For both SAz-1 and SWy-1, the molar absorptivity of the 920-cm^{-1} band showed the greatest dehydration dependence. For example, the ϵ_{920} value of Ca-SAz-1 decreases from 90 to 55 cm^2 mmol$_{OH}^{-1}$ upon dehydration. Similar decreases were observed for all cations with Ca^{2+} showing the largest effect. The molar absorptivity of the 885-cm^{-1} band of SWy-1 also decreased significantly upon lowering the H_2O content. This band is less intense than the 920-cm^{-1} band and occurs only in SWy-1. For both SAz-1 and SWy-1, the 840–845-cm^{-1} band, which is assigned to the

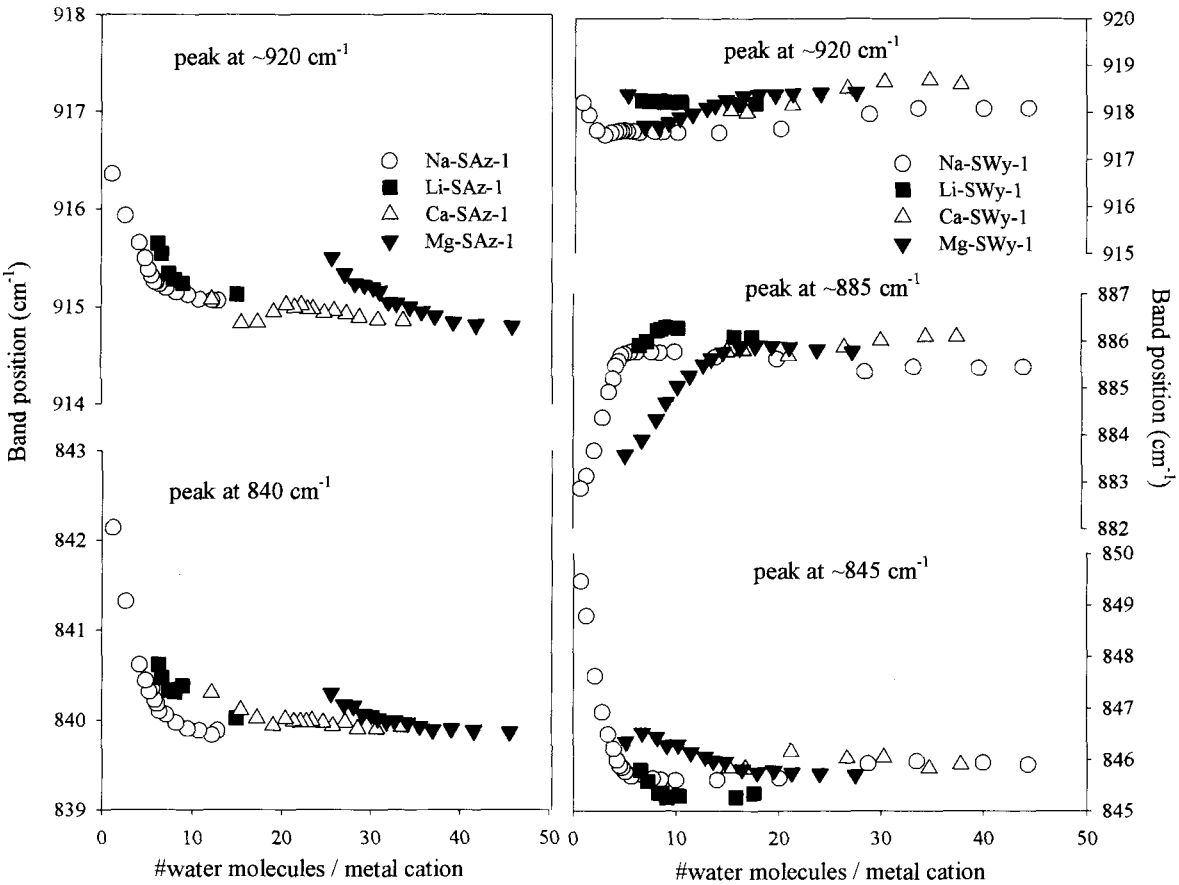

Figure 7. Positions of the structural OH-bending vibrations of Na-, Li-, Ca-, and Mg-exchanged SAz-1 (left side) and SWy-1 (right side) montmorillonite as a function of H_2O content.

$AlFe^{3+}OH$ group, showed the smallest dehydration-dependent reduction in molar absorptivity.

For SAz-1, the changes in molar absorptivity of the structural OH-bending vibrations for the Na- and Li-exchanged forms were similar to each other and were distinct from the Ca- and Mg-exchanged samples. For Na- and Li-exchanged SAz-1, the molar absorptivity of the 920 and 840-cm^{-1} bands decreased upon lowering the H_2O content to <6 H_2O molecules per exchangeable cation. A similar trend was observed for the Ca- and Mg-SAz-1 samples, but the transition point occurred at a H_2O content of ~20 water molecules per exchangeable cation.

DISCUSSION

Sorption isotherms

The shape of the isotherms shown in Figure 2 generally reflects the hydration characteristics of the exchangeable cations. The data presented in Figure 2 show that little hysteresis is observed for the more strongly hydrated cations (Mg^{2+} and Ca^{2+}). Significantly greater hysteresis was observed for Na-SAz-1. This difference is in agreement with previous water-vapor sorption studies (Mooney *et al.,* 1952a, 1952b; Keren and Shainberg, 1975; Berend *et al.,* 1996). The more strongly hydrated cations Mg^{2+} and Ca^{2+} retain more interlayer H_2O molecules at low relative pressure of water vapor than the Na-exchanged clays (Figure 2). As shown by Suquet *et al.* (1975), Na-exchanged saponite, beidellite, and hectorite collapse to a *d*(001)-value of 1.0 nm. In contrast, the lowest *d*(001)-value reported for the same clays exchanged with Ca was 1.2 nm. Thus, the hydrated interlayer Ca^{2+} and Mg^{2+} cations are molecular "props" to keep the layers separated. For Na-exchanged SAz-1 and especially for the lower-charged SWy-1, the layers collapse at low relative pressure of water vapor. Increased hysteresis is attributed to the energy requirements to reexpand the layers from 1.0 to 1.2 nm.

As noted by Cases *et al.* (1997), the shapes of the adsorption-desorption isotherms are complex and cannot be assigned to a standard isotherm shape. A general feature, however, is that the amount of H_2O sorbed at low-H_2O contents (relative vapor pressure $p/p_o < 0.4$) is influenced largely by the hydration energy of the exchangeable cation. In a combined sorption and

https://doi.org/10.1346/CCMN.2000.0480115 Published online by Cambridge University Press

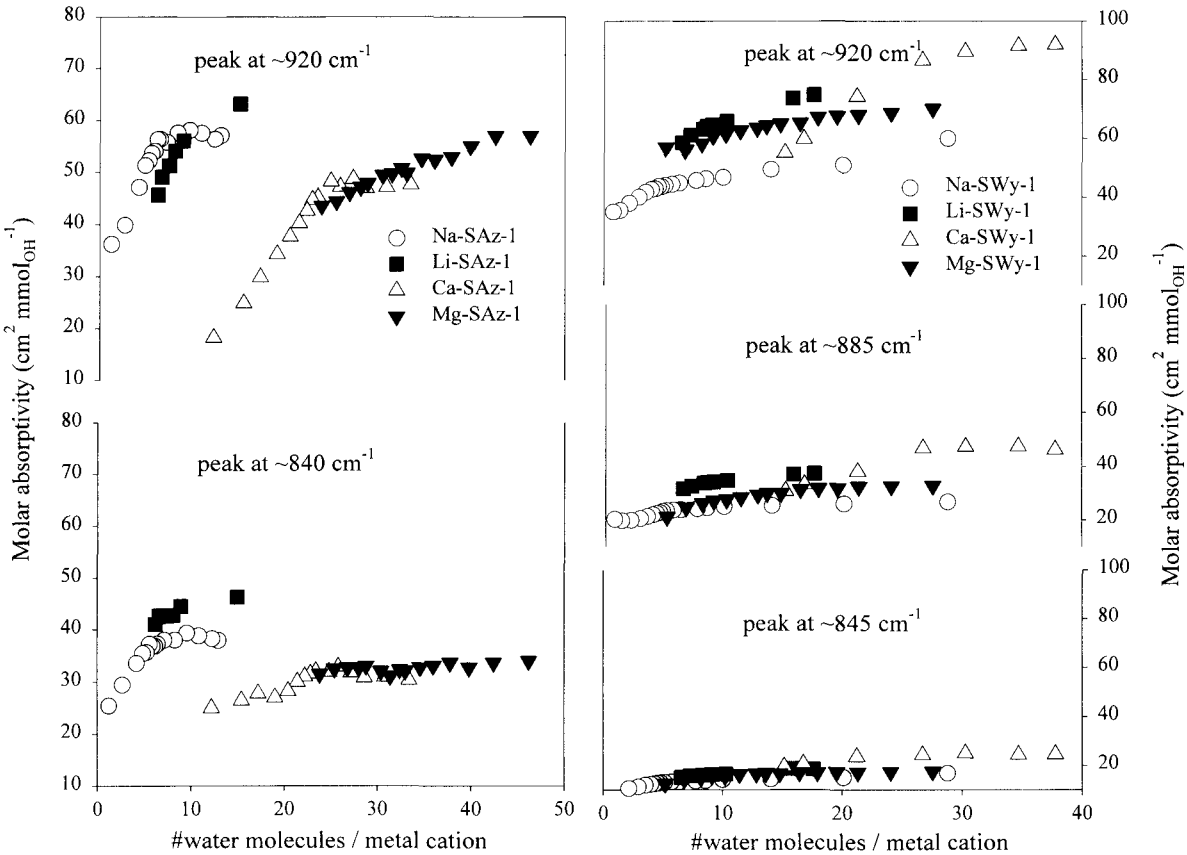

Figure 8. Molar absorptivities (cm^2 $mmol_{OH}^{-1}$) of the structural OH-bending vibrations of Na-, Li-, Ca-, and Mg-exchanged SAz-1 (left side) and SWy-1 (right side) montmorillonite as a function of H_2O content.

microcalorimeter study, a similar relationship was observed by Cancela *et al.* (1997) who showed that the amount of H_2O sorbed by smectite was positively correlated with the hydration energy of the exchangeable cation. In addition, water-vapor adsorption isotherms for Na-, K-, Cs-, and Ca-exchanged SAz-1 were reported recently by Chiou and Rutherford (1997).

A unique advantage of the EIRM cell for determination of water-vapor sorption isotherms is that the dry mass of the sample can be determined directly without complete desiccation. Using the EIRM cell, the absorbance of the H_2O-bending and/or stretching bands can be correlated directly to the amount of H_2O sorbed to the clay. Thus, the dry mass of the self-supporting film can be obtained by extrapolation of the intensity of the H-O-H bending band of water *vs.* mass curve. This avoids excessive drying of the sample, which may ultimately influence the water-sorption characteristics of the clay.

Vibrational properties of sorbed H_2O

Upon lowering the H_2O content of the smectite-H_2O complexes, the H-O-H bending band shifts to a lower frequency, the O-H stretching bands of H_2O shift to higher frequencies, and the molar absorptivity of the H-O-H bending band increases. These observations are in agreement with Poinsignon *et al.* (1978). At low-H_2O contents of $\leq$3 H_2O molecules per exchangeable cation, the asymmetric OH-stretching, symmetric OH-stretching, and H-O-H bending frequencies of H_2O sorbed to hectorites were 3635, 3571, and 1626.5 cm^{-1} (Poinsignon *et al.*, 1978). Lower-H_2O contents were achieved by Poinsignon *et al.* (1978) than the values obtained here because the samples were subjected to vacuum and mild heating. Nonetheless, the positions of the H_2O bands in this study tend toward the lower-H_2O content values obtained by Poinsignon *et al.* (1978). In both studies, the positions of these vibrational bands of water are shifted relative to their positions in bulk H_2O. Although IR spectroscopy "samples" all of the water molecules present in the sample, the spectra obtained at low-water content values of <10 H_2O molecules/cation are dominated by water molecules that are closely associated with the exchangeable cations and the charged portions of the interlamellar surface. At high-H_2O contents (p/p_o > 0.7), the positions of the H_2O-vibrational bands are similar to those of bulk H_2O. The position of the

https://doi.org/10.1346/CCMN.2000.0480115 Published online by Cambridge University Press

ν_1(OH) band for Mg-SWy-1 occurs at a slightly lower value of 3403 cm^{-1} compared to 3413 cm^{-1} for Mg-SAz-1. This small change in frequency is consistent with weak hydrogen bonding occurring at the interlayer surface associated with tetrahedral sites of SWy-1 exhibiting substitution (Yariv, 1992a).

Upon desorption, H_2O molecules sorbed on the external surfaces of the clay and H_2O within interstitial pores are selectively removed from the clay; H_2O molecules associated with exchangeable cations are more difficult to remove because of the large hydration energies associated with the interlayer cations. These cation-associated H_2O molecules are characterized by higher ν(OH) and lower δ(HOH) frequencies. According to Sposito and Prost (1982), the first stage of water adsorption by smectites is the solvation of exchangeable cations followed by sorption in interstitial pores and external surfaces. Similarly, in a model developed by Yariv (1992a, 1992b), H_2O molecules occur in one of three zones, each with a different H_2O arrangement. Zone A_m and zone A_o represent H_2O molecules coordinated to interlayer cations and to the siloxane surface, respectively. Zone B_{om} has a disordered H_2O arrangement between the ordered zones A_m and A_o. During the dehydration process, H_2O molecules in the B_{om} zone, in interstitial pores, and on external surfaces are preferentially removed from the clay. In our study, the remaining H_2O molecules are assigned to zone A_m. Our study does not show a clear distinction between H_2O molecules of zone A_m and zone A_o. In particular, at low-water contents of <10 H_2O molecules per exchangeable cation, both the negative charge on the siloxane surface (Yariv, 1992a) and the positive charge of the exchangeable cation affects the structure of H_2O in the interlayer.

As hydrogen bonding increases, the positions of the OH-stretching bonds shift to lower frequencies and the δ(HOH) mode of H_2O shifts to higher frequency (Pimentel and McClellan, 1960). The increase in frequency of the ν(OH) bands of H_2O and the concomitant decrease in frequency of the δ(HOH) band of H_2O provide direct evidence that H_2O sorbed to the clay at water contents of <10 H_2O molecules per exchangeable cation is less hydrogen bonded than that of bulk H_2O. Upon lowering the H_2O content of the smectite-H_2O complex, the H_2O molecules are clustered around the exchangeable cations. These coordinated H_2O molecules are restricted in their ability to form hydrogen bonds with adjacent H_2O molecules.

Yan *et al.* (1996a, 1996b) suggested that the structure of interlayer H_2O is affected mainly by the formation of hydrogen bonds between H_2O molecules and the siloxane surface. Experimentally, they reported that the position of the ν_2 mode of H_2O decreased upon lowering the H_2O content for Na- and Li-exchanged montmorillonite, which is in agreement with the data reported here and Russell and Farmer (1964), Poinsignon *et al.* (1978), and Johnston *et al.* (1992, 1997). Yan *et al.* (1996a, 1996b) interpreted the decrease in frequency of the ν_2 band to a coupling between H_2O molecules and the Si-O stretching vibrations of the 2:1 layer through the formation of hydrogen bonds. The shift of the ν_2 mode to lower frequency, however, is not consistent with this interpretation or with the observed blue-shift of the ν(OH) modes of sorbed H_2O reported here. Our results indicate that H_2O is less hydrogen bonded at low-H_2O content. H_2O molecules clustered around exchangeable cations are polarized by the close proximity to the exchangeable cation with the oxygen of the H_2O directed toward the metal cation. Thus, a decrease in hydrogen bonding is consistent with isolated hydrated clusters of metal cations at the interlayer surface.

The larger molar absorptivity of H_2O coordinated to exchangeable cations can distinguish bulk H_2O from H_2O surrounding exchangeable cations. Upon desorption of H_2O from the interlayer surface, the molar absorptivity increases until a water content of 4–6 H_2O molecules per exchangeable cation is reached. At this water content, the d(001)-value of the smectite is $\sim$1.26 nm, which corresponds to a one-layer smectite hydrate (Farmer, 1978). The H_2O present at the interlayer under these conditions is essentially all coordinated to exchangeable cations in the interlayer and is characterized by a significantly greater molar-absorptivity value compared to bulk H_2O. Upon further desorption, collapse of the interlayer occurs with a decrease in the d(001)-value to $\sim$1.0 nm (Farmer, 1978).

Reintroduction of water to the dry Na-exchanged clay results in an initial *decrease* in molar absorptivity (Figure 5). For Na-SWy-1, at a H_2O content of 2 H_2O molecules per exchangeable cation, the adsorbed H_2O is characterized by a molar absorptivity similar to that of bulk H_2O. This indicates that the initial H_2O sorbed on the clay is not present in the interlayer, but on external surfaces of the clay. When a critical H_2O content of $\sim$4 H_2O molecules per exchangeable cation is reached, sufficient H_2O is present to allow the intercalation of H_2O in the interlayer of the clay. Less hysteresis is observed for the higher-charged Na-SAz-1 than for Na-SWy-1. Apparently, the higher density of interlayer cations in SAz-1 serves to hold the layers apart. When water vapor is reintroduced to SAz-1, H_2O can readily be intercalated into the interlayer. The main conclusion from the hysteresis in molar absorptivity is that the mechanism of H_2O desorption is distinct from that of adsorption.

Smectite

In good agreement with IR studies of reduced-charge montmorillonite (Calvet and Prost, 1971; Sposito *et al.*, 1983; Madejova *et al.*, 1996), our results indicate that the structural OH-bending vibrations were influenced by H_2O content. The structural OH

https://doi.org/10.1346/CCMN.2000.0480115 Published online by Cambridge University Press

groups of montmorillonite reside within the 2:1 layer at the base of the siloxane ditrigonal cavity. The observed spectral perturbation of both the frequency and molar absorptivity of these structural OH groups provide spectroscopic evidence that the local environment around OH groups is influenced by the keying of H_2O and by the exchangeable cation.

Small frequency shifts of <5 wavenumbers were observed for the structural OH-bending vibrations upon changes in H_2O content. Least affected was the 920-cm^{-1} band, which is assigned to the AlAlOH group. For SWy-1, the 885-cm^{-1} band decreased in frequency whereas the 845-cm^{-1} band *increased* in frequency with a lower-H_2O content. Unlike the 920-cm^{-1} band, the bands at 885 and 845 cm^{-1} correspond to sites of isomorphic substitution within the 2:1 layer. Because of the negative charge associated with these sites, exchangeable cations will reside near siloxane ditrigonal cavities. The change in frequency of these bands is assigned to perturbations by the exchangeable cation. Upon lowering H_2O content, the interlayers collapse and exchangeable cations enter into the siloxane ditrigonal cavities, which perturb the structural OH groups at the base of the cavity. However, it is not clear why the positions of the AlFeOH and AlMgOH groups shift in opposing directions.

In contrast to the change in frequency of the structural OH groups, the 920-cm^{-1} band is most affected by molar absorptivity and lowering H_2O content. This band is assigned to the AlAlOH group. In agreement with Calvet and Prost (1971) and Prost *et al.* (1981), the intensity of the 920-cm^{-1} band is sharply decreased at low-H_2O content. Unlike the 885 and 840-cm^{-1} bands, this band is associated with "neutral" siloxane ditrigonal cavities where no isomorphous substitution occurs near the cavity. There are two plausible explanations for the reduction in molar absorptivity of the AlAlOH group. First, the reduction in intensity may result from polarization effects induced by the exchangeable cation or H_2O located near the ditrigonal cavities. Second, because the samples are well-oriented self-supporting films with clay particles aligned with *c* axes perpendicular to the surface of the film, the change in intensity may result from H_2O molecules and/or exchangeable cations penetrating into the ditrigonal cavities to cause the orientation of the structural OH group to tilt out of the (001) plane. This would effectively reduce the IR cross section of these OH groups. An intriguing aspect of such changes to the structural OH groups is that they provide a site-specific reporter group to examine H_2O-H_2O and cation interactions with the surface at the interlayer. The AlAlOH groups provide information about the neutral portion of the surface at the interlayer whereas the 885 and 840-cm^{-1} bands provide information about the negatively charged sites in the clay structure. Upon collapse, the interlayer cations are in close proximity to two siloxane ditrigonal cavities. Presumably, at least one of the siloxane ditrigonal cavities will bear a negative charge resulting from isomorphous substitution. Because of the low net negative charge on the 2:1 layers, it is doubtful that the opposing ditrigonal cavity is negatively charged. Thus, a single cation may influence both charged (*i.e.,* 885 and 840 cm^{-1}) and neutral (*i.e.,* 920 cm^{-1}) OH-deformation bands upon partial collapse.

Despite the recessed location of the structural OH group, H_2O molecules and exchangeable cations have the ability to influence both the position and molar absorptivity of these groups. Spectral perturbations of this hydroxyl group were reported by Serratosa *et al.* (1984) for intercalated smectites. They showed that certain types of organic amines were oriented with the NH_3^+ end perpendicular to [001]. These amines perturbed the stretching band of the structural OH group of vermiculite. In a related study, Johnston and Stone (1990) showed that hydrazine can key into the siloxane ditrigonal cavity of the kaolinite-hydrazine complex, thereby perturbing the stretching vibration of the inner OH group.

ACKNOWLEDGMENTS

Financial support for this work was provided, in part, by the U.S. Department of Agriculture National Research Initiative program. In addition, the authors thank G. Sposito, J.L. White, and reviewers W. Carey, S. Yariv, and I. Lapides for helpful comments during the review process.

REFERENCES

Alba, M.D., Alvero, R., Becerro, A.I., Castro, M.A., and Trillo, J.M. (1998) Chemical behavior of lithium ions in reexpanded Li-montmorillonites. *Journal of Physical Chemistry B,* **102,** 2207–2213.

Bérend, I., Cases, J.M., François, M., Uriot, J.P., Michot, L., Masion, A., and Thomas, F. (1996) Mechanism of adsorption and desorption of water vapor by homoionic montmorillonites: 2. The Li^+ Na^+, K^+, Rb^+ and Cs^+-exchanged forms. *Clays and Clay Minerals.* **43,** 324–336.

Breen, C., Madejova, J., and Komadel, P. (1995) Characterisation of moderately acid-treated, size-fractionated montmorillonites using IR and MAS NMR Spectroscopy and thermal analysis. *Journal of Materials Chemistry,* **5,** 469–474.

Calvet, R. and Prost, R. (1971) Cation migration into empty octahedral sites and surface properties of clays. *Clays and Clay Minerals,* **19,** 175–186.

Cancela, G.D., Huertas, F.J., Taboada, E.R., Sanchez Rasero, F., and Laguna, A.H. (1997) Adsorption of water vapor by homoionic montmorillonites. Heats of adsorption and desorption. *Journal of Colloid and Interface Science,* **185,** 343–354.

Cases, J.M., Bérend, I., Besson, G., François, M., Uriot, J.P., Thomas, F., and Poirier, J.E. (1992) Mechanism of adsorption and desorption of water vapor by homoionic montmorillonite. 1. The sodium exchanged form. *Langmuir,* **8,** 2730–2739.

Cases, J.M., Bérend, I., François, M., Uriot, J.P., Michot, L.J., and Thomas, F. (1997) Mechanism of adsorption and desorption of water vapor by homoionic montmorillonite. 3.

The Mg^{2+}, Ca^{2+}, Sr^{2+} and Ba^{2+} exchanged forms. *Clays and Clay Minerals,* **45,** 8–22.

Chang, F.R.C., Skipper, N.T., and Sposito, G. (1997) Monte Carlo and molecular dynamics simulations of interfacial structure in lithium-montmorillonite hydrates. *Langmuir,* **13,** 2074–2082.

Chiou, C.T. and Rutherford, D.W. (1997) Effects of exchanged cation and layer charge on the sorption of water and EGME vapors on montmorillonite clays. *Clays and Clay Minerals,* **45,** 867–880.

Farmer, V.C. (1974) The Layer Silicates. In *The Infrared Spectra of Minerals,* V.C. Farmer, ed., The Mineralogical Society, London, 331–359.

Farmer, V.C. (1978) Water on particle surfaces. In *Chemistry of Soil Constituents,* D.J. Greenland and M.H.B. Hayes, eds., Wiley, New York, 405–448.

Johnston, C.T. and Aohci, Y.O. (1996) Fourier transform infrared and Raman spectroscopy. In *Methods of Soil Analysis Part 3 Chemical Methods,* D.L. Sparks, ed., Soil Science Society of America, Madison, Wisconsin, 269–321.

Johnston, C.T. and Stone, D.A. (1990) Influence of hydrazine on the vibrational modes of kaolinite. *Clays and Clay Minerals,* **38,** 121–128.

Johnston, C.T., Tipton, T., Stone, D.A., Erickson, C., and Trabue, S.L. (1991) Chemisorption of p-dimethoxybenzene on Cu-montmorillonite. *Langmuir,* **7,** 289–296.

Johnston, C.T., Sposito, G., and Erickson, C. (1992) Vibrational probe studies of water interactions with montmorillonite. *Clays and Clay Minerals,* **40,** 722–730.

Johnston, C.T., Xu, W., Parker, P., and Agnew, S.F. (1998) Characterization of active sites on mineral surfaces: An infrared study of water sorption on montmorillonte. In *The Latest Frontiers of Clay Chemistry: Proceedings of the Sapporo Conference on the Chemistry of Clays and Clay Minerals,* A. Yamagishi, A. Aramata, and M. Taniguchi, eds., The Smectite Forum of Japan, Sapporo, 47–69.

Karaborni, S., Smit, B., Heidug, W., Urai, J., and van Oort, E. (1996) The swelling of clays: Molecular simulations of the hydration of montmorillonite. *Science,* **271,** 1102–1104.

Keren, R. and Shainberg, I. (1975) Water vapor isotherms and heat of immersion of Na/Ca-montmorillonite systems - I: Homoionic clay. *Clays and Clay Minerals,* **23,** 193–200.

Kijne, J.W. (1969) On the interaction of water molecules and montmorillonite surfaces. *Soil Science Society of America Proceedings,* **33,** 539–543.

Madejova, J., Bujdak, J., Gates, W.P., and Komadel, P. (1996) Preparation and infrared spectroscopic characterization of reduced-charge montmorillonite with various Li contents. *Clay Minerals,* **31,** 233–241.

Mooney, R.W., Keenan, A.G., and Wood, L.A. (1952a) Adsorption of water vapor by montmorillonite. I. Heat of desorption and application of BET theory. *Journal of the American Chemical Society,* **74,** 1367–1370.

Mooney, R.W., Keenan, A.G., and Wood, L.A. (1952b) Adsorption of water vapor by montmorillonite. II. Effect of exchangeable ions and lattice swelling as measured by X-ray diffraction. *Journal of the American Chemical Society,* **74,** 1371–1374.

Mortland, M.M. and Raman, K.V. (1968) Surface acidities of smectites in relation to hydration, exchangeable-cation and structure. *Clays and Clay Minerals,* **16,** 393–398.

Pimentel, G.C. and McClellan, A.B. (1960) *The Hydrogen Bond, 1st edition,* W.H. Freeman and Co., San Fransisco, 475 pp.

Poinsignon, C., Cases, J.M., and Fripiat, J.J. (1978) Electrical-polarization of water molecules adsorbed by smectites. An infrared study. *Journal of Physical Chemistry,* **82,** 1855–1860.

Russell, J.D. and Farmer, V.C. (1964) Infra-red spectroscopic study of the dehydration of montmorillonite and saponite. *Clay Minerals Bulletin,* **5,** 443–464.

Serratosa, J.M., Rausell-Colom, J.A., and Sanz, J. (1984) Charge-density and its distribution in phyllosilicates: Effect on the arrangement and reactivity of adsorbed species. *Journal of Molecular Catalysis,* **27,** 223–234.

Skipper, N.T., Refson, K., and McConnell, J.D.C. (1991) Computer simulation of interlayer water in 2:1 clays. *Journal of Chemical Physics,* **94,** 7434–7445.

Skipper, N.T., Chang, F.R.C., and Sposito, G. (1995a) Monte-Carlo simulation of interlayer molecular structure in swelling clay minerals. 1. Methodology. *Clays and Clay Minerals,* **43,** 285–293.

Skipper, N.T., Sposito, G., and Chang, F.R.C. (1995b) Monte Carlo simulation of interlayer molecular structure in swelling clay minerals. 2. Monolayer hydrates. *Clays and Clay Minerals,* **43,** 294–303.

Sposito, G. and Prost, R. (1982) Structure of water adsorbed on smectites. *Chemistry Review,* **82,** 553–573.

Sposito, G., Prost, R., and Gaultier, J.P. (1983) Infrared spectroscopic study of adsorbed water on reduced-charge Na/Li montmorillonites. *Clays and Clay Minerals,* **31,** 9–16.

Suqute, H., Calle, C.D.I., and Pezerat, H. (1975) Swelling and structural organization of saponite. *Clays and Clay Minerals,* **23,** 1–9.

Tipton, T., Johnston, C.T., Trabue, S.L., Erickson, C., and Stone, D.A. (1993) Gravimetric/FTIR apparatus for the study of vapor sorption on clay films. *Review of Scientific Instruments,* **64,** 1091–1092.

van Olphen, H. and Fripiat, J.J. (1979) *Data Handbook for Clay Materials and Other Non-Metallic Minerals, 1st edition,* Pergamon Press, Oxford, 346 pp.

Venyaminov, S.Y. and Prendergast, F.G. (1997) Water (H_2O and D_2O) molar absorptivity in the 1000–4000 cm^{-1} range and quantitative infrared spectroscopy of aqueous solutions. *Analytical Biochemistry,* **248,** 234–245.

Weaver, C.E. and Pollard, L.D. (1973) *The Chemistry of Clay Minerals,* Elsevier Scientific Publishing Co., Amsterdam, 213 pp.

Yan, L., Roth, C.B. and Low, P.F. (1996a) Changes in the Si-O vibrations of smectite layers accompanying the sorption of interlayer water. *Langmuir,* **12,** 4421–4429.

Yan, L., Low, P.F., and Roth, C.B. (1996b) Swelling pressure of montmorillonite layers versus H-O-H bending frequency of the interlayer water. *Clays and Clay Minerals,* **44,** 749–756.

Yariv, S. (1992a) The effect of tetrahedral substitution of Si by Al on the surface acidity of the oxygen plane of clay minerals. *International Reviews in Physical Chemistry,* **11,** 345–375.

Yariv, S. (1992b) Wettability of clay minerals. In *Modern Approaches to Wettability: Theory and Applications.* M.E. Schrader and G. Loeb, eds., Plenum Press, New York, 279–326.

E-mail of corresponding author: clays@purdue.edu

(Received 21 September 1998; accepted 17 August 1999; Ms. 98-115)